

# Adaptive Non-Uniform Sampling of Bandlimited Signals via Algorithm–Encoder Co-Design

Kaluguri Yashaswini\*, Anshu Arora\* *Student Member, IEEE* and Satish Mulleti *Member, IEEE*

**Abstract**—We propose an adaptive non-uniform sampling framework for bandlimited signals based on an algorithm–encoder co-design perspective. By revisiting the convergence analysis of iterative reconstruction algorithms for non-uniform measurements, we derive a local, energy-based sufficient condition that governs reconstruction behavior as a function of the signal and derivative energies within each sampling interval. Unlike classical approaches that impose a global Nyquist-type bound on the inter-sample spacing, the proposed condition permits large gaps in slowly varying regions while enforcing denser sampling only where the signal exhibits rapid temporal variation. Building on this theoretical insight, we design a variable-bias, variable-threshold integrate-and-fire time encoding machine (VBT-IF-TEM) whose firing mechanism is explicitly shaped to enforce the derived local convergence condition. To ensure robustness, a shifted-signal formulation is introduced to suppress excessive firing in regions where the magnitude of the signal amplitude is close to zero or the local signal energy approaches zero. Using the proposed encoder, an analog signal is discretely represented by time encodings and signal averages, enabling perfect reconstruction via a standard iterative algorithm even when the local sampling rate falls below the Nyquist rate. Simulation results on synthetic signals and experiments on ultrasonic guided-wave and ECG signals demonstrate that the proposed framework achieves substantial reductions in sampling density compared to uniform sampling and conventional IF-TEMs, while maintaining accurate reconstruction. The results further highlight a controllable tradeoff between sampling density, reconstruction accuracy, and convergence behavior, which can be navigated through adaptive parameter selection.

**Index Terms**—Adaptive non-uniform sampling, time encoding machines, integrate-and-fire models, iterative reconstruction, bandlimited signals, event-based sampling, algorithm–encoder co-design.

## I. INTRODUCTION

**S**AMPLING theory lies at the heart of modern signal processing and underpins a wide range of technologies, including digital communications, biomedical signal acquisition, imaging systems, and sensing platforms. By providing a principled bridge between continuous-time physical signals and their discrete-time digital representations, sampling theory enables a reliable signal acquisition, processing, storage, and transmission. Classical results such as the Shannon–Nyquist sampling theorem establishes fundamental conditions under which continuous-time signals can be perfectly reconstructed from discrete measurements and continue to guide the design of practical sampling and acquisition systems [1], [2].

\* Equal contribution

The authors are with the Department of Electrical Engineering, Indian Institute of Technology (IIT) Bombay, Mumbai, India. Emails: yashkaluguri2005@gmail.com, anshuarora2604@gmail.com, mulleti.satish@gmail.com

Consider a real-valued, finite-energy signal  $f(t)$  belonging to the class of bandlimited signals  $\mathcal{B}_{\Omega_0, c}$ , that is,

$$\mathcal{B}_{\Omega_0, c} \triangleq \{f(t) \in L^2(\mathbb{R}) : F(\omega) = 0 \text{ for } |\omega| > \Omega_0, |f(t)| \leq c\}, \quad (1)$$

where  $F(\omega)$  denotes the Fourier transform of  $f(t)$ . According to the Shannon–Nyquist sampling theorem, any signal  $f(t) \in \mathcal{B}_{\Omega_0, c}$  can be perfectly reconstructed from its uniform samples  $\{f(nT_s)\}_{n \in \mathbb{Z}}$  provided that

$$T_s \leq T_{\text{Nyq}} \triangleq \frac{\pi}{\Omega_0}. \quad (2)$$

While this condition guarantees perfect reconstruction, the sampling rate is dictated by the *maximum* frequency content of the signal, and is therefore governed by the worst-case temporal variation.

In many practical scenarios, bandlimited signals exhibit strong temporal nonuniformity: rapid variations occur only over short intervals, while the signal remains slowly varying or nearly flat for most of the observation duration. Examples include biomedical signals, acoustic signals, and ultrasonic guided-wave measurements. Uniform sampling at the Nyquist rate in such cases leads to significant redundancy, motivating the study of non-uniform and adaptive sampling schemes. For example, in nuclear magnetic resonance spectrography and magnetic resonance imaging, the measurements can be non-uniform, and densities are defined a priori to achieve specific objectives [3], [4].

In non-uniform sampling (NUS), the signal is measured at a set of known time instants  $\Lambda = \{t_n\}_{n \in \mathbb{Z}}$ , producing samples  $\{f(t_n)\}$ . Classical results show that  $f(t)$  can be uniquely determined from  $\{f(t_n)\}$  provided the sampling set satisfies a density condition, commonly expressed in terms of the lower Beurling density [5]

$$D^-(\Lambda) \triangleq \liminf_{T \rightarrow \infty} \inf_{t \in \mathbb{R}} \frac{|\Lambda \cap [t, t+T]|}{T} \geq \frac{\Omega_0}{\pi}. \quad (3)$$

However, uniqueness alone is insufficient in practice. Most reconstruction algorithms for bandlimited signals—particularly iterative methods—require stronger, algorithm-dependent conditions to guarantee stability and convergence. Let

$$T_n = t_{n+1} - t_n, \quad (4)$$

and denote  $T_{\max} = \sup_n T_n$ . In order to ensure the convergence of the commonly used iterative reconstruction algorithms, it is typically required that

$$T_n \leq T_{\max} < T_{\text{Nyq}}, \quad (5)$$

as shown in [6]–[10]. As a result, even non-uniform sampling schemes remain effectively constrained by a *global Nyquist-type bound*, limiting their ability to exploit local variations.

An alternative sampling paradigm is offered by *time encoding machines* (TEMs), which represent signals through the timing of events rather than amplitude samples [10]–[26]. In particular, integrate-and-fire TEMs (IF-TEMs) generate time encodings/firings<sup>1</sup>  $\{t_n\}$  by recording the instants at which the integral of a biased signal crosses a fixed threshold  $\Delta$ , that is,

$$\int_{t_n}^{t_{n+1}} (f(t) + b) dt = \Delta, \quad (6)$$

where  $b > c$  ensures positivity of the integrand. This mechanism yields an event-driven sampling scheme whose firing rate increases with signal amplitude. Under suitable choices of  $(b, \Delta)$ , perfect reconstruction of bandlimited signals from the resulting time encodings has been established.

Despite their advantages, conventional IF-TEMs suffer from two fundamental limitations that lead to oversampling. First, the firing rate is primarily governed by the signal amplitude rather than by its local temporal variation. Second, the existing reconstruction guarantees require the inter-firing intervals  $T_n$  to satisfy a global Nyquist-type upper bound.

These observations point to a broader limitation of existing approaches: sampling mechanisms and reconstruction algorithms are typically designed and analyzed in isolation. In contrast, the convergence behavior of iterative reconstruction algorithms is governed by local properties of the signal, suggesting that sampling strategies should be explicitly designed to enforce these convergence requirements. This motivates an *algorithm–encoder co-design* perspective, in which the sampling process is shaped to satisfy the requirements of the reconstruction algorithm itself.

Within this perspective, we ask the following question: *Is it possible to design an adaptive sampling scheme for bandlimited signals in which the sampling density follows local signal variation, while still guaranteeing perfect reconstruction without enforcing a global Nyquist-type gap constraint?*

In this work, we answer this question by adopting a co-design approach that revisits the convergence analysis of iterative reconstruction algorithms for bandlimited signals acquired from non-uniform measurements. Instead of imposing a uniform bound on  $T_n$ , we derive a *local, energy-based sufficient condition* for convergence that depends on the energies of the signal and its derivative over each sampling interval. This condition permits large inter-sample gaps in slowly varying regions while enforcing denser sampling only where the signal exhibits rapid changes.

Building on this theoretical insight, we design a *variable-bias, variable-threshold integrate-and-fire time encoding machine (VBT-IF-TEM)* whose bias and threshold are adapted as functions of local signal energies. The resulting firing mechanism produces time encodings that are sparse in low-variation regions and dense during rapid transitions. To prevent excessive firing in low-energy regimes—specifically when the

<sup>1</sup>Throughout the paper, the terms *time encodings*, *firings*, and *samples* are used interchangeably.

magnitude of the signal amplitude is small, or the local signal energy is low (that is,  $|f(t)| \approx 0$ )—we introduce a shifted-signal formulation that ensures stable, robust, and practically implementable sampling behavior.

Using the proposed VBT-IF-TEM as a core building block, we develop an adaptive non-uniform sampling framework in which an analog signal is discretely represented as  $\{t_n, y_n\}_{n \in \mathbb{Z}}$ , where  $t_n$  are time encodings and

$$y_n = \int_{t_n}^{t_{n+1}} f(t) dt, \quad (7)$$

are signal averages. We show that the original bandlimited signal can be perfectly reconstructed from  $\{t_n, y_n\}_{n \in \mathbb{Z}}$  using an iterative reconstruction algorithm, even when the inter-sample spacing locally exceeds the Nyquist interval. Importantly, this does not violate the Nyquist sampling theorem; rather, it replaces a global sufficient condition with a locally adaptive sufficient condition for perfect reconstruction.

The main contributions (Section II) of this work are summarized as follows.

- We derive a *local, energy-based sufficient condition* for the convergence of iterative reconstruction algorithms for bandlimited signals from non-uniform samples, replacing the classical global Nyquist gap constraint with a signal-dependent bound (cf. Section II-A).
- We adopt an *algorithm–encoder co-design* perspective and develop a signal-dependent time-encoding mechanism based on a VBT-IF-TEM model, whose firing behavior is explicitly designed to enforce the derived local convergence condition (cf. Section II-B). Importantly, the resulting sampling rates adapt to the local signal variation rather than signal amplitude.
- To ensure practical robustness, we introduce a *shifted-signal formulation* that suppresses excessive firing in regions of low signal amplitude magnitude or low local energy, while preserving perfect reconstruction guarantees (cf. Section II-C).
- We establish that *perfect reconstruction* of bandlimited signals is possible even when the inter-sample spacing locally exceeds the Nyquist interval, with theoretical guarantees formalized in Theorems 1, 2, and 3.
- Through simulations on synthetic signals and experiments on real-world data, including ultrasonic guided-wave and ECG signals, we demonstrate substantial reductions in sampling density compared to uniform sampling and conventional IF-TEMs, while maintaining accurate reconstruction (cf. Sections III and V). Additionally, the results highlight a tradeoff between the number of samples and reconstruction accuracy.
- Finally, we present a simple *adaptive parameter selection strategy* that dynamically switches between high- and low-rate sampling regimes based on instantaneous signal activity, further reducing sampling redundancy (cf. Section IV).

## II. ADAPTIVE NON-UNIFORM SAMPLING APPROACH

In this section, we present an adaptive non-uniform sampling framework in which a bandlimited signal is represented

by a set of time encodings and corresponding measurements. The key idea is to generate time encodings that are dense in regions where the signal varies rapidly and sparse in regions where the signal varies slowly.

This section is organized as follows. First, we review the conventional iterative reconstruction algorithm used in the IF-TEM framework and revisit its convergence analysis. In doing so, we derive an alternative convergence condition that does not require the classical Nyquist inter-sample spacing constraint in (5). Next, we introduce the proposed VBT-IF-TEM, which serves as a key building block for the adaptive sampling framework. We then discuss the limitations of this formulation and present a modified variant that addresses these issues. Finally, we combine these elements to formulate the proposed adaptive non-uniform sampling scheme.

### A. Iterative Reconstruction and Convergence Analysis

In this subsection, we revisit the iterative reconstruction algorithm commonly used in the IF-TEM framework and examine its convergence properties in detail. Our objective is to identify the fundamental bottleneck that enforces a Nyquist-type sampling constraint and to reformulate this condition in a manner that enables locally adaptive sampling.

To proceed, consider the IF-TEM framework described in the previous section. From (6), signal averages are determined from the time encodings  $\{t_n\}$  and the TEM parameters as

$$y_n = \int_{t_n}^{t_{n+1}} f(t) dt = \Delta - b(t_{n+1} - t_n). \quad (8)$$

To reconstruct the signal from the time encodings or the averages  $\{y_n\}$ , an iterative reconstruction process is applied [10]. The process uses an operator  $\mathcal{A}$  defined as

$$\mathcal{A}f(t) = \sum_{n \in \mathbb{Z}} y_n g(t - s_n) \quad (9)$$

where  $g(t) = \frac{\sin(\Omega_0 t)}{\pi t}$  is a sinc function and  $s_n = \frac{t_{n+1} + t_n}{2}$  denotes the midpoint between consecutive firings.

Let  $f_l(t)$ ,  $l \in \mathbb{N}$ , be a sequence of bandlimited functions generated by the recursion

$$f_{l+1} = f_l + \mathcal{A}(f - f_l) \quad (10)$$

with the initial condition  $f_0 = \mathcal{A}f$ . If

$$\|\mathcal{I} - \mathcal{A}\| \leq \alpha, \quad (11)$$

where  $\mathcal{I}$  denotes the identity operator, then it follows that

$$\|f - f_l\| \leq \alpha^{l+1} \|f\|. \quad (12)$$

Consequently, if  $\alpha < 1$ , the recursion converges and

$$\lim_{l \rightarrow \infty} f_l(t) = f(t). \quad (13)$$

We now examine the convergence proof in more detail to identify precisely where a Nyquist-type sampling constraint arises. For convergence, it suffices to show that

$$\|\mathcal{I}f - \mathcal{A}f\|^2 \leq \alpha^2 \|f\|^2, \quad (14)$$

for all  $f \in \mathcal{B}_{\Omega_0, c}$  with  $\alpha < 1$ . A key step in the proof relies on Wirtinger's inequality (cf. Appendix B in [10]), applied to the partial norm  $\int_{t_n}^{t_{n+1}} |f(t) - f(s_n)|^2 dt$ . This yields the bound

$$\int_{t_n}^{t_{n+1}} |f(t) - f(s_n)|^2 dt \leq \frac{T_n^2}{\pi^2} \int_{t_n}^{t_{n+1}} |f'(t)|^2 dt. \quad (15)$$

Summing over all firing intervals and using the uniform bound  $T_n \leq T_{\max}$  gives

$$\sum_{n \in \mathbb{Z}} \int_{t_n}^{t_{n+1}} |f(t) - f(s_n)|^2 dt = \|\mathcal{I}f - \mathcal{A}^*f\|^2 \leq \frac{T_{\max}^2}{\pi^2} \|f'\|^2, \quad (16)$$

where  $\mathcal{A}^*$  denotes the adjoint of  $\mathcal{A}$ , and  $f'$  is the first-derivative of  $f$ . Applying Bernstein's inequality  $\|f'\|^2 \leq \Omega_0^2 \|f\|^2$  and using  $\|\mathcal{A}\| = \|\mathcal{A}^*\|$ , we obtain

$$\|\mathcal{I}f - \mathcal{A}f\|^2 \leq \left( \frac{T_{\max} \Omega_0}{\pi} \right)^2 \|f\|^2. \quad (17)$$

This implies  $\alpha = \frac{T_{\max} \Omega_0}{\pi}$ , and therefore convergence requires  $T_{\max} < T_{\text{Nyq}} = \frac{\pi}{\Omega_0}$ . This condition explains why existing reconstruction guarantees enforce a sampling rate above the Nyquist rate.

To relax this global constraint, we next introduce the following quantities:

$$e_n(t) = \int_t^t |f(u)|^2 du, \quad d_n(t) = \int_t^t |f'(u)|^2 du, \quad (18)$$

and define  $E_n = e_n(t_{n+1})$  and  $D_n = d_n(t_{n+1})$  as the energies of the signal and derivative, respectively, over the interval  $T_n$ .

With this notation, the right-hand side of (15) can be expressed as  $\frac{T_n^2}{\pi^2} D_n$ . For convergence, it is sufficient that

$$\sum_{n \in \mathbb{Z}} \frac{T_n^2}{\pi^2} D_n \leq \alpha \sum_{n \in \mathbb{Z}} E_n, \quad (19)$$

for some  $\alpha < 1$ . A sufficient local condition ensuring this inequality is  $\frac{T_n^2}{\pi^2} D_n < E_n$ , which equivalently yields

$$T_n < \pi \sqrt{\frac{E_n}{D_n}}. \quad (20)$$

This condition reveals that larger inter-sample gaps are permissible in regions where the signal variation is small, while denser sampling is required when the derivative energy is large compared to the signal's energy. Consequently, the inter-sample spacing  $T_n$  may locally exceed the Nyquist interval in slowly varying regions without compromising convergence.

In the following, we design a variable-bias, variable-threshold IF-TEM that generates time encodings satisfying the local convergence condition in (20), thereby enabling adaptive non-uniform sampling with perfect reconstruction guarantees.

### B. Variable-Bias-Threshold IF-TEM

Figure 1 illustrates the proposed variable-bias-threshold IF-TEM framework. After each firing at time  $t_n$ , the bias and threshold are updated to  $b_n(t)$  and  $\Delta_n(t)$ , respectively, such that  $b_n(t) + f(t) > 0$  and  $\Delta_n(t) > 0$  for all  $t \in [t_n, t_{n+1}]$ .

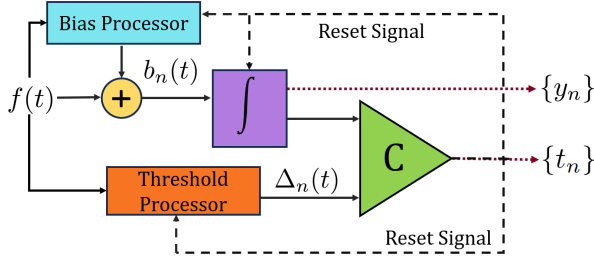


Fig. 1: Framework of the proposed VBT-IF-TEM

Following the firing at  $t_n$  and the subsequent integrator reset, the signal  $f(t) + b_n(t)$  is integrated and compared against the threshold  $\Delta_n(t)$ . The next firing time  $t_{n+1}$  therefore satisfies

$$\int_{t_n}^{t_{n+1}} (f(t) + b_n(t)) dt = \Delta_n(t_{n+1}). \quad (21)$$

We now examine how the encoding interval  $T_n = t_{n+1} - t_n$  can be controlled within this framework. This analysis directly informs the design of the bias and threshold functions to achieve the desired signal-dependent sampling pattern while ensuring convergence of the iterative reconstruction algorithm.

Since the local convergence condition in (20) requires an upper bound on  $T_n$ , we focus on bounding the inter-firing interval generated by the VBT-IF-TEM in Fig. 1. The firing interval is maximized when the integrand  $f(t) + b_n(t)$  attains its minimum value. Let  $b_{n,\min} = \min_{t \in [t_n, t_{n+1}]} b_n(t)$ . Then, by noting that  $-c \leq f(t)$  for all  $t$ , we obtain

$$T_n \leq \frac{\Delta_n(t_{n+1})}{b_{n,\min} - c}. \quad (22)$$

Unlike the upper bound in a conventional IF-TEM, which is given by  $\Delta/(b-c)$  and remains constant across firing intervals, the bound in (22) varies with  $n$ . By equating this bound to the local convergence condition in (20), we obtain signal-dependent time encodings that enable perfect reconstruction.

The following theorem summarizes the first main result of this section.

**Theorem 1.** *Let  $f(t) \in \mathcal{B}_{\Omega_0, c}$  be a bandlimited signal. Consider a variable-bias-threshold IF-TEM sampling as shown in Fig. 1. The signal can be perfectly reconstructed from the time encodings  $\{t_n\}$  generated by the approach, provided that the bias and thresholds are chosen as follows:*

$$b_n(t) = c + \frac{1}{\pi\sqrt{\alpha e_n(t)}}, \quad \Delta_n(t) = \frac{1}{\sqrt{d_n(t) + \beta e_n(t)}}, \quad (23)$$

where  $\alpha \in (0, 1)$  and  $\beta > 0$  are user-defined positive scalars.

*Proof.* To prove the theorem, let us first focus on the minimum value of the bias  $b_n(t)$ . Since  $e_n(t)$  is monotonically increasing, the bias is a decreasing function, and its minimum value occurs at  $t = t_{n+1}$ . Hence,  $b_{n,\min} = c + \frac{1}{\sqrt{\alpha E_n}}$ . Next, consider the upper bound on  $T_n$  in (22). For the choices of

bias and threshold, the bound is given as

$$T_n \leq \frac{\Delta_n(t_{n+1})}{b_{n,\min} - c} = \pi \sqrt{\frac{\alpha E_n}{D_n + \beta E_n}} < \pi \sqrt{\frac{E_n}{D_n}}, \quad (24)$$

where the last inequality stems from the fact that  $D_n + \beta E_n > D_n$ , and  $0 < \alpha < 1$ . Hence, the proposed sampling scheme results in signal-variation-dependent encodings that also satisfy the desired condition for the iterative algorithm to converge.  $\square$

For reconstruction, the iterative algorithm uses the signal averages, which can be expressed using (21) as

$$y_n = \int_{t_n}^{t_{n+1}} f(t) dt = \Delta_n(t_{n+1}) - \int_{t_n}^{t_{n+1}} b_n(t) dt. \quad (25)$$

Here are a few remarks regarding the implications of Theorem 1.

**Remark 1.** *No explicit upper bound is imposed on the maximum gap between firing instances. In other words,  $T_n$  may exceed  $T_{Nyq}$ , unlike in conventional sampling and IF-TEM approaches. The admissible magnitude of  $T_n$  depends on the local signal variations captured by  $E_n$  and  $D_n$ .*

**Remark 2.** *To illustrate the dependence of the firing rate on signal variation, consider a single-tone signal  $f(t) = A_0 \cos(\Omega_m t)$ , where  $A_0 \leq c$  and  $\Omega_m \leq \Omega_0$ . Although this signal is not of finite energy, it serves as a useful example for understanding firing behavior. For this signal,  $e_n(t)$  and  $d_n(t)$  are given by*

$$e_n(t) = A_0^2 \frac{t - t_n}{2} + A_0^2 \frac{\sin 2\Omega_m t - \sin 2\Omega_m t_n}{4\Omega_m} \quad (26)$$

$$d_n(t) = A_0^2 \Omega_m^2 \frac{t - t_n}{2} - A_0^2 \Omega_m^2 \frac{\sin 2\Omega_m t - \sin 2\Omega_m t_n}{4\Omega_m}$$

We regard the signal as varying rapidly when the product  $A_0 \Omega_m$  is large. This is intuitive: increasing either the amplitude or the frequency results in faster signal variations. Substituting (26) into (23), we observe that for a fixed frequency, increasing the amplitude decreases both the bias and the threshold, with the threshold decreasing more rapidly. This leads to smaller inter-firing intervals  $T_n$  and hence a higher firing rate. Similarly, for a fixed amplitude, increasing the frequency decreases the threshold and increases the firing rate. These observations confirm that the proposed firing mechanism adapts to local signal variation.

**The Oversampling Issue:** Despite these desirable properties, the proposed formulation may result in excessive firing when the signal exhibits negligible variation. In particular, when the magnitude of the signal amplitude is very small, both  $b_n(t)$  and  $\Delta_n(t)$  grow large, with the bias term increasing more rapidly than the threshold. This behavior can result in frequent firings even in regions where the local energy satisfies  $e_n(t) \approx 0$ , which is equivalent to  $|f(t)| \approx 0$ .

To mitigate this issue, one may consider introducing regularization constants into the bias and threshold definitions to prevent unbounded growth. For example, consider the

modified choices

$$\begin{aligned} b_n(t) &= c + \frac{1}{\pi \sqrt{\alpha e_n(t) + \gamma_1^2}}, \\ \Delta_n(t) &= \frac{1}{\sqrt{d_n(t) + \beta e_n(t) + \gamma_2^2}}, \end{aligned} \quad (27)$$

where  $\gamma_1, \gamma_2 > 0$ . Under this modification, when the signal variation is negligible, the bias and threshold approach the finite values  $c + 1/\gamma_1$  and  $1/\gamma_2$ , respectively. As a result, the firing interval in such regions is bounded by  $T_n \leq \frac{\gamma_1}{\gamma_2(c\gamma_1+1)}$ . For a fixed  $\gamma_1$ , choosing a small value of  $\gamma_2$  keeps the threshold large and leads to sparse firing in low-amplitude regions.

However, it is not immediately clear whether these modified bias and threshold functions preserve the perfect reconstruction guarantees established earlier. In the following subsection, we propose a principled solution that resolves this issue.

### C. VBT-IF-TEM with Biased Signal

To address the oversampling behavior discussed in the previous subsection, which arises primarily when the local energy term  $e_n(t)$  becomes very small, we introduce a constant shift  $s > c$  to the signal  $f(t)$  such that  $f(t) + s > 0$  for all  $t$ . Specifically, we define the shifted signal  $\tilde{f}(t) = f(t) + s$ , and correspondingly introduce the energies of the shifted signal and its derivative as

$$\tilde{e}_n(t) = \int_{t_n}^t |\tilde{f}(u)|^2 du, \quad \text{and} \quad \tilde{d}_n(t) = \int_{t_n}^t |\tilde{f}'(u)|^2 du, \quad (28)$$

respectively, with  $\tilde{E}_n = \tilde{e}_n(t_{n+1})$  and  $\tilde{D}_n = \tilde{d}_n(t_{n+1})$ .

Since  $\tilde{f}(t) > 0$  by construction, it follows that  $\tilde{e}_n(t) > 0$  for all  $t > t_n$ . Consequently, the bias term  $b_n(t)$  and the threshold  $\Delta_n(t)$ , as defined in (29), remain finite for all sampling intervals. This shifted-signal formulation, therefore, effectively mitigates excessive firing in low-energy regimes while preserving the theoretical guarantees of the sampling framework.

The following theorem summarizes the main theoretical result of this paper.

**Theorem 2.** *Let  $f(t) \in \mathcal{B}_{\Omega_0, c}$  be a bandlimited signal. Consider a variable-bias-threshold IF-TEM sampling as shown in Fig. 1. The signal can be perfectly reconstructed from the time encodings generated by the approach, provided that the bias and thresholds are chosen as follows:*

$$b_n(t) = c - s + \frac{1}{\pi \sqrt{\alpha \tilde{e}_n(t)}}, \quad \Delta_n(t) = \frac{1}{\sqrt{\tilde{d}_n(t) + \beta \tilde{e}_n(t)}}, \quad (29)$$

where  $\alpha \in (0, 1)$  and  $\beta > 0$  are user-defined positive scalars.

*Proof.* To prove the theorem, let us first focus on the minimum value of the bias  $b_n(t)$ . Since  $\tilde{E}_n(t)$  is monotonically increasing, the bias is a decreasing function, and its minimum value occurs at  $t = t_{n+1}$ . Hence,  $b_{n,\min} = c - s + \frac{1}{\sqrt{\alpha \tilde{E}_n}}$ .

Also, since  $\tilde{f}(t) > s - c$ , the upper bound on  $T_n$  is  $\frac{\Delta_n(t_{n+1})}{b_{n,\min} + s - c}$ . For the choices of bias and threshold, the bound is given as

$$T_n \leq \frac{\Delta_n(t_{n+1})}{b_{n,\min} + s - c} = \pi \sqrt{\frac{\alpha \tilde{E}_n}{\tilde{D}_n + \beta \tilde{E}_n}} < \pi \sqrt{\frac{\tilde{E}_n}{\tilde{D}_n}}, \quad (30)$$

where the last inequality stems from the fact that  $\tilde{D}_n + \beta \tilde{E}_n > \tilde{D}_n$ , and  $0 < \alpha < 1$ . Hence, we now have

$$\|\tilde{f} - \mathcal{A}\tilde{f}\|^2 \leq \alpha \|\tilde{f}\|^2. \quad (31)$$

We note that this provides reconstruction guarantees for  $\tilde{f}(t)$ ; however, by definition, removing the constant offset  $s$  allows us to perfectly recover  $f(t)$  from the time encodings.  $\square$

With the additional signal shift, the proposed sampling scheme retains all the desirable properties established in Theorem 1, while avoiding excessive firing when the signal amplitude is small. This behavior can be verified by reconsidering the single-tone example discussed in Remark 2. To further illustrate the effect of the signal shift, Fig. 2 compares the firing patterns of the VBT-IF-TEM with and without the shift for a representative bandlimited signal. We note that the firings have been reduced from 396 to 51 by adding a bias.

As anticipated from the analysis in Remark 2, the unshifted formulation exhibits excessive firing in low-energy regimes, particularly in regions where the magnitude of the signal amplitude is small. In contrast, introducing the shift controls the growth of the bias term  $b_n(t)$ , thereby significantly reducing the firing rate in such regions while preserving dense sampling in regions of high signal variation.

To further elucidate the behavior of the proposed scheme and to quantify the dependence of the firing rate in response to signal variation, we consider the following two representative scenarios.

- *Signal with low variation:* In this case, both the signal and its derivative are negligible over the interval  $T_n$ . Mathematically, this corresponds to  $\tilde{D}_n \rightarrow 0$  and  $f(t) \rightarrow 0$ , which implies  $\tilde{f}(t) \rightarrow s$ . Substituting into (30), we obtain

$$T_n^{\text{Low}} \leq \pi \sqrt{\frac{\alpha}{\beta}} = T_{\max}. \quad (32)$$

This bound indicates that when the signal variation is negligible, the firing intervals are large and can be controlled through appropriate choices of  $\alpha$  and  $\beta$ .

- *Signal with large variation:* In this scenario, both the signal amplitude and its derivative are significant. Specifically, we consider  $\tilde{f}'(t) \rightarrow c\Omega_0$  and  $f(t) \rightarrow c$ , which implies  $\tilde{f}(t) \rightarrow s + c$ . Substituting into (30), we obtain

$$\begin{aligned} T_n^{\text{High}} &\leq \pi \sqrt{\frac{\alpha(s+c)^2}{\beta(s+c)^2 + (c\Omega_0)^2}}, \\ &\leq \pi \sqrt{\frac{\alpha}{\beta}} \sqrt{\frac{(s+c)^2 \beta}{(c\Omega_0)^2 + (s+c)^2 \beta}}. \end{aligned} \quad (33)$$

Here,  $T_n^{\text{High}}$  denotes the inter-firing interval in regions of high signal variation.

The upper bound in the high-variation regime is tighter than that in the low-variation case, which is consistent

with the desired behavior of increased firing density during rapid signal changes. Moreover, the bounds in (32) and (33) can be controlled through suitable choices of  $\alpha$ ,  $\beta$ , and  $s$ , providing explicit tuning of the sampling density across different signal regimes.

With the biased VBT-IF-TEM, the local convergence condition is satisfied, and excessive firing is effectively suppressed in low-energy regimes where the magnitude of the signal amplitude is small. We then formalize an adaptive non-uniform sampling representation based on the resulting time encodings and signal averages.

#### D. Proposed Adaptive Non-Uniform Sampling

The proposed non-uniform sampling approach is built upon the VBT-IF-TEM framework discussed in the previous subsections. The output of the TEM consists of the time encodings  $\{t_n\}$ . However, for signal reconstruction using the iterative algorithm, the signal averages  $\{y_n\}$  in (25) are also required.

In a conventional IF-TEM with constant bias and threshold, the signal averages can be recovered from the time encodings using (6) as  $\Delta - b(t_{n+1} - t_n)$ . In contrast, when the bias and threshold vary across firing intervals, recovering the averages during reconstruction requires knowledge of the corresponding bias and threshold functions. To avoid this additional overhead, we compute and store the signal averages directly during the encoding process as shown in Fig. 1. This leads to the following result.

**Theorem 3** (Adaptive Non-Uniform Sampling). *Let  $f(t) \in \mathcal{B}_{\Omega_0, c}$  be a bandlimited signal, and let  $\{t_n\}$  denote the time encodings generated using the VBT-IF-TEM with biased signal as in Theorem 2. Then the signal can be discretely represented as  $\{y_n, t_n\}_{n \in \mathbb{Z}}$ , where the signal averages  $y_n$  are determined using (25). Moreover, the signal can be perfectly reconstructed from these discrete measurements using the standard iterative reconstruction algorithm.*

While the VBT-IF-TEM produces only time encodings, the proposed adaptive non-uniform sampling framework additionally encodes signal averages; this distinction enables reconstruction using the discrete representation  $\{t_n, y_n\}$ .

To gain further insight into the proposed adaptive sampling strategy, we analyze its behavior on a representative signal exhibiting four distinct regions of variation, as illustrated in Fig. 3. This example allows us to examine how the firing rate, computed as  $1/T_n$ , adapts to changes in signal amplitude and local frequency content. As expected, the firing rate remains low in regions of low amplitude and low variation, and increases significantly as the signal amplitude and local frequency increase. Notably, in certain regions, the firing rate falls below the Nyquist rate without compromising perfect reconstruction. In this example, the sampling parameters used are  $\alpha = 0.7$ ,  $\beta = 2450$ ,  $c = 1$ , and  $s = 3c$ . The proposed method uses 95 samples, compared to 90 samples required by uniform sampling at the Nyquist rate, and the resulting reconstruction achieves a normalized mean squared error (NMSE) of  $-52.24$  dB.

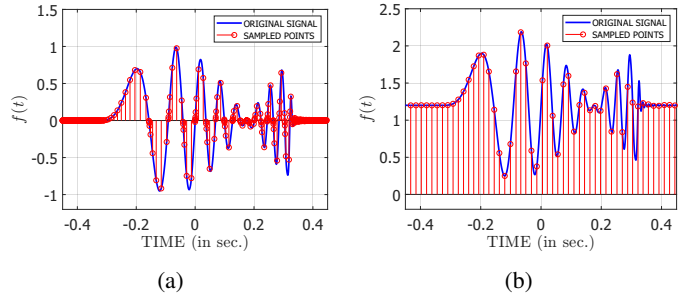


Fig. 2: A comparison of firings of VBT-IF-TEMs (a) without shift – 396 firings, and (b) with shift – 51 firings.

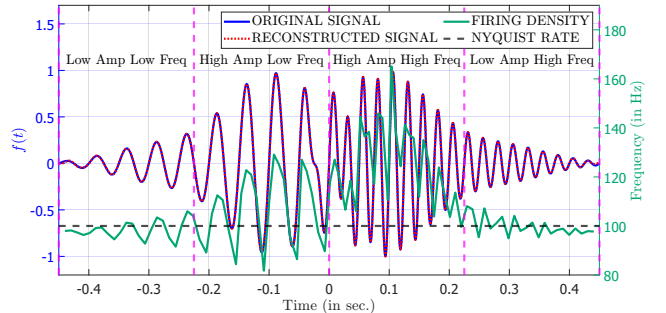


Fig. 3: Different firing rates in different regions

#### E. Related Work

In this subsection, we position the proposed framework within the broader literature on non-uniform sampling and reconstruction of bandlimited signals, with an emphasis on the theoretical convergence guarantees established in Theorems 1, 2, and 3.

*Irregular sampling and reconstruction:* Early work on irregular sampling primarily focused on the *sampling jitter* model, where uniform sampling locations are perturbed by small timing errors [27]–[29]. A seminal contribution by Duffin and Schaeffer [27] established a frame-based reconstruction framework for such sampling patterns. Subsequent works extended these ideas to more general non-uniform sampling sets and iterative reconstruction algorithms [7], [30]; see [31] for a comprehensive review.

Several studies have also considered reconstruction from *signal averages* rather than pointwise samples [30]–[33], which forms the mathematical basis for IF-TEM reconstruction. In these approaches, convergence of the iterative algorithm is guaranteed under a global Nyquist-type constraint on the maximum inter-sample spacing, as expressed in (5). A related line of work investigates accelerating convergence by oversampling, showing that enforcing  $T_{\max} < T_{\text{Nyq}}/m$  yields a convergence factor of  $\alpha^m$ , where  $m \in \mathbb{N}$  [7], [30], [34].

*Adaptive and signal-dependent sampling:* Adaptive sampling schemes based on *level crossings* have been widely studied, wherein samples are acquired at time instants when the signal crosses predefined amplitude levels [35]–[40]. For a fixed set of levels  $\{\Delta_k\}_{k=1}^K$ , the signal is represented by time instants  $\{t_{k,n}\}$  satisfying  $f(t_{k,n}) = \Delta_k$ . While increasing the number of levels results in denser sampling, the sampling den-

sity depends strongly on the level placement within the signal's dynamic range. Although the uniqueness of reconstruction can be ensured when the crossing density exceeds the Nyquist rate [35], [38], explicit conditions ensuring convergence of iterative reconstruction algorithms—particularly guarantees analogous to (5)—remain largely unexplored.

In practice, when a signal remains between two successive levels for extended durations, inter-sample gaps may become arbitrarily large. Whether such sampling patterns satisfy the requirements for stable reconstruction is generally unclear. Some works attempt to regulate the crossing density by adding auxiliary signals, such as ramps [41], but a systematic link between signal variation and reconstruction guarantees remains missing.

*Nonlinear transformations and varying-bandwidth models:* Alternative approaches to non-uniform sampling include nonlinear transformations [42], [43] and models with time-varying bandwidth [44]–[47]. For example, [42] proposes a nonlinear mapping that converts non-uniform samples  $\{f(t_n)\}$  into uniform samples of a transformed bandlimited signal. Similarly, time-varying bandwidth models allow local adaptation of sampling density. However, these methods rely on restrictive signal models or transformations, limiting their applicability. In contrast, the proposed framework applies to all bandlimited signals without imposing additional structural assumptions.

*IF-TEM with variable bias:* Recent works on IF-TEMs with variable bias have demonstrated that adapting the bias can reduce oversampling relative to fixed-bias designs, while the firing rate remains primarily proportional to the signal amplitude [48], [49]. In contrast, the present work generalizes the IF-TEM paradigm by jointly adapting both the bias and the threshold as functions of local signal energies. This design explicitly links firing behavior to signal variation and is theoretically grounded in local convergence guarantees for iterative reconstruction.

*Summary:* In summary, while prior work has addressed irregular sampling, adaptive acquisition, and IF-TEM encoding from different perspectives, the proposed framework uniquely integrates a local, energy-based convergence analysis with signal-dependent time encoding. This integration enables adaptive non-uniform sampling with rigorous reconstruction guarantees that do not rely on a global Nyquist-type constraint.

### III. SIMULATION RESULTS

In this section, we compare the proposed adaptive non-uniform sampling method with two baseline approaches: (i) uniform sampling at or above the Nyquist rate, and (ii) a conventional IF-TEM (C-IF-TEM) with fixed bias and threshold. For all methods, signal reconstruction is performed using signal averages and the iterative reconstruction algorithm described earlier.

In all experiments, we consider bandlimited signals with finite temporal support, such that the signal is negligible outside the observation interval. Performance is evaluated in

terms of the number of samples ( $\#S$ ) and the normalized mean-squared error (NMSE), defined as

$$\text{NMSE (in dB)} = 10 \log \frac{\|f(t) - \hat{f}(t)\|^2}{\|f(t)\|^2}, \quad (34)$$

where  $\hat{f}(t)$  denotes the reconstructed signal. For reconstruction and NMSE evaluation, both  $f(t)$  and  $\hat{f}(t)$  are evaluated on a fine uniform time grid.

We consider two classes of bandlimited signals: a chirp-like signal and a sum-of-sincs (SoS) signal. These signal classes capture key characteristics of practical signals, including strong temporal nonuniformity and localized regions of high variation.

#### A. Chirp Signal

We first consider a chirp-like bandlimited signal, which is particularly well-suited for demonstrating the benefits of adaptive sampling. Such signals exhibit pronounced *temporal nonuniformity*, consisting of extended intervals of slow variation interspersed with short bursts of rapid change. This structure allows sparse sampling in low-activity regions, while the rapidly varying segments dictate the overall bandwidth.

The test signal is constructed as a bandlimited waveform via sinc interpolation, where the interpolation coefficients are modulated by a slowly varying envelope multiplied by a nonlinear chirp. This results in localized bursts of high temporal variation within an otherwise smooth signal. Specifically, the signal is generated as

$$\begin{aligned} f(t) &= \sum_{m=1}^M c_m \text{sinc}\left(2F_0\left(t - mT_s + \frac{M}{2}T_s\right)\right), \quad (35) \\ F_0 &= 100 \text{ Hz}, \quad T_s = \frac{1}{2F_0}, \quad M = 130, \\ c_m &= \sin(2\pi \times 0.005 m) \sin\left(2\pi \times 0.081 \frac{m^{2.1}}{2M}\right), \\ t &\in [-T_{\max}, T_{\max}], \quad T_{\max} = 0.45 \text{ s}. \end{aligned}$$

By definition,  $\text{sinc}(x) = \sin(\pi x)/(\pi x)$ , and the signal amplitude is normalized to satisfy  $|f(t)| \leq c = 1$ . For this experiment, the parameters of the proposed method are set to  $\alpha = 0.5$ ,  $\beta = 5600$ , and  $s = 4.2$ , while  $b = 1.3$  and  $\Delta = 0.0015$  were chosen for the C-IF-TEM. These parameters are selected to yield the lowest NMSE for each method.

Fig. 4 compares the reconstruction results and sampling patterns obtained using uniform sampling, C-IF-TEM, and the proposed adaptive method. We point out that, in all our experiments, the reconstruction used for uniform sampling is sinc interpolation, and the iterative reconstruction method is used for the other two sampling schemes. Several observations can be made. First, all methods achieve high reconstruction accuracy, with NMSE values below  $-50$  dB. Second, both uniform sampling and the proposed method require substantially fewer samples than C-IF-TEM. Third, the sampling density of the proposed method adapts to the local signal variation and can fall below the Nyquist rate in low-activity regions.

Within the observation interval, the proposed method uses 169 samples, compared to 180 samples required by uniform

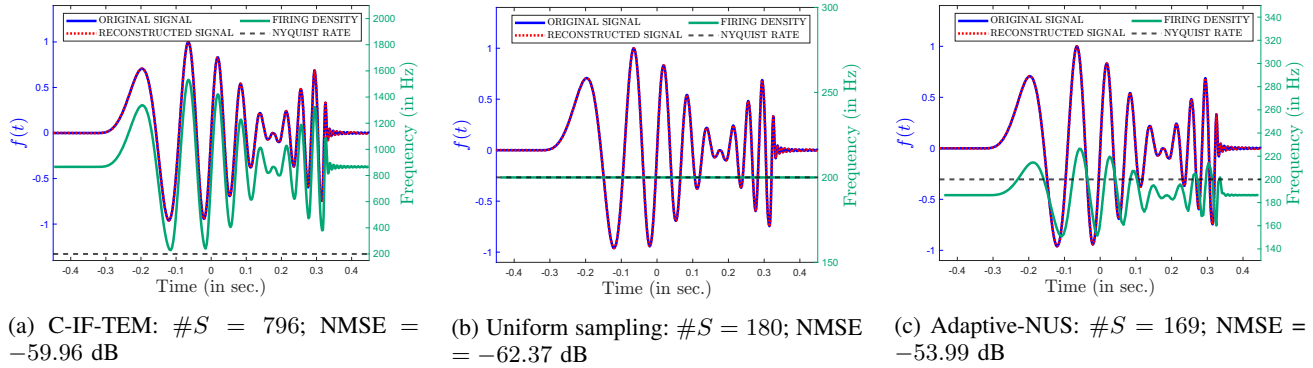


Fig. 4: Comparison of different sampling schemes for a chirp-like signal. The proposed Adaptive-NUS produces fewer samples and achieves sub-Nyquist sampling in low-activity regions.

Nyquist sampling. In practice, the proposed method requires storing both time encodings and signal averages, resulting in  $2 \times 169$  measurements. This modest increase in measurement count comes with the advantage of eliminating the need for a global clock and the ability to sample below the Nyquist rate in extended low-activity regions, which can yield significant savings in applications characterized by sparse signal activity.

### B. Sum-of-Sincs Signal

We next evaluate the proposed method using a sum-of-sincs (SoS) signal, which provides a natural and flexible representation of bandlimited signals. This formulation enables the construction of signals with multiple regions of distinct bandwidths and varying degrees of temporal activity.

For the simulations, the signal is generated as a non-overlapping linear combination of sinc functions with different bandwidths, given by

$$f(t) = f_1(t) + f_2(t - \tau) + f_2(t + \tau), \quad (36)$$

where

$$f_k(t) = \sum_{n=-N_k}^{N_k} c_{k,n} \text{sinc}(2F_k(t - nT_k)), \text{ for } k = \{1, 2\},$$

with  $T_1 = 0.6$  ms,  $T_2 = 0.4$  ms,  $\tau = 0.15$  s,  $N_1 = 50$ ,  $N_2 = 100$ ,  $c_{k,n} \sim \text{Uniform}(-0.5, 0.5)$ ,  $F_1 = 50$  Hz,  $F_2 = 20$  Hz. The resulting signal is normalized to unit amplitude and truncated to the interval  $[-0.45, 0.45]$  s. It consists of three distinct regions: the first and last segments are dominated by slowly varying components with a bandwidth 20 Hz, while the middle segment is a faster signal with a bandwidth 50 Hz.

Fig. 5 shows the signal, its reconstructions, and the corresponding firing patterns. Consistent with the chirp experiment, the proposed method's sampling density increases with the local signal's amplitude and frequency content. We use the parameters of the proposed method are set to  $\alpha = 0.45$ ,  $\beta = 2400$ , and  $s = 3$ , while the C-IF-TEM parameters are chosen as  $b = 1.2$  and  $\Delta = 0.0015$ .

To obtain statistically meaningful results, we evaluate the methods over 100 independent SoS signals. The average NMSEs and sampling rates are reported in Table I, and closely match the behavior observed in individual trials.

TABLE I: Comparison of sampling strategies

| Sampling Type       | Number of Samples | NMSE Error (dB) |
|---------------------|-------------------|-----------------|
| Uniform Sampling    | 90                | -44.76          |
| Conventional IF-TEM | 731               | -55.70          |
| Adaptive-NUS        | 96                | -59.74          |

We next examine the convergence behavior of the iterative reconstruction algorithm. Since the proposed method relies on locally adaptive convergence conditions rather than a global bound, a slower convergence rate is expected compared to C-IF-TEM. Fig. 6 shows the average NMSE across 100 SoS signals as a function of iteration count.

As anticipated, the proposed method requires more iterations to converge. However, this increased iteration count is accompanied by a substantial reduction in the number of samples. Specifically, C-IF-TEM requires approximately 731 samples on average, whereas the proposed method achieves comparable reconstruction accuracy with only about 96 samples on average. Increasing the number of iterations beyond the values shown in Fig. 6 does not alter the final reconstruction error, confirming that the observed behavior reflects a tradeoff between sampling density and convergence speed rather than a loss of reconstruction fidelity.

Finally, we investigate the effect of the hyperparameters  $\alpha$  and  $\beta$  on performance. Fig. 7 shows the average NMSE and number of samples across 100 signals for different parameter choices. Larger values of  $\beta$  and smaller values of  $\alpha$  generally yield lower NMSE, but at the cost of increased sampling density.

These results highlight a fundamental tradeoff between reconstruction accuracy and the number of samples. In the next section, we explore whether this trade-off can be further improved through adaptive parameter selection.

### IV. ADAPTIVE SELECTION OF $\alpha$ AND $\beta$

In this section, we present a simple adaptive mechanism for selecting the parameters  $\alpha$  and  $\beta$  in the proposed adaptive non-uniform sampling (or VBT-IF-TEM) framework. The objective is to demonstrate how adaptive parameter selection can further improve sampling efficiency by aligning the sampling density with the instantaneous behavior of the signal.

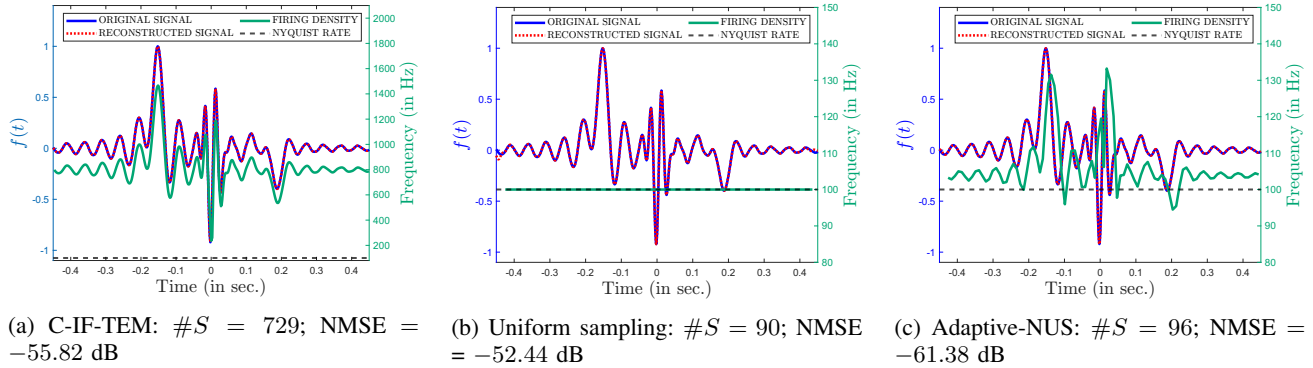


Fig. 5: Comparison of different sampling schemes for a SoS signal with multiple bandwidth regions. The proposed Adaptive-NUS produces fewer samples and achieves sub-Nyquist sampling in low-activity regions.

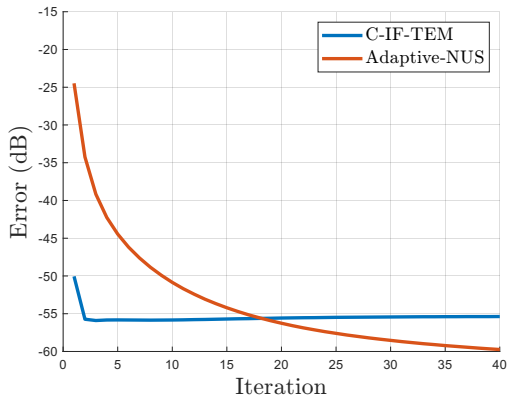


Fig. 6: NMSE across 100 SoS signals versus iteration count for the iterative reconstruction algorithm.

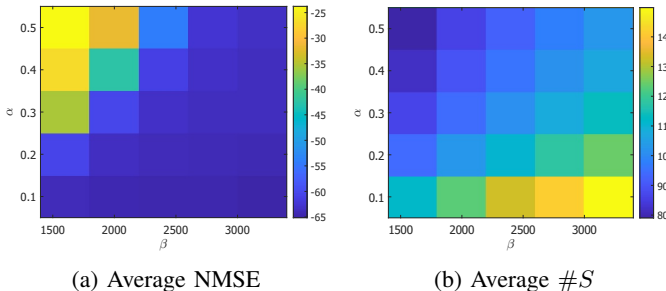


Fig. 7: Heatmaps of average NMSE and number of samples across 100 SoS signals, illustrating the tradeoff between reconstruction accuracy and sampling density as functions of  $\{\alpha, \beta\}$ .

As indicated by the inter-sample interval bounds in (32) and (33), the sampling behavior of the proposed scheme is explicitly governed by the parameters  $\alpha$  and  $\beta$ . Increasing  $\alpha$  relaxes the admissible inter-sample interval and reduces the number of generated samples, whereas increasing  $\beta$  tightens this bound and leads to a higher sampling density. This intrinsic tradeoff can be exploited to design a more adaptive and robust sampling mechanism that responds to local signal characteristics, thereby reducing the overall sampling burden while maintaining reconstruction accuracy.

In many practical signals, large temporal regions exhibit little variation. While the current approach demonstrates strong performance, the use of fixed sampling parameters  $(\alpha, \beta)$  over the full signal duration results in sampling of low-variation regions, contributing to additional redundancy and an increased sample count.

To further enhance performance, we propose a *two-level adaptive sampling strategy* in which the parameters  $(\alpha, \beta)$  are adjusted online based on instantaneous signal activity. We emphasize that this strategy represents only one possible approach for adapting  $\alpha$  and  $\beta$ ; alternative adaptation rules, switching criteria, or multi-level extensions can be developed depending on the signal characteristics and application requirements. The present formulation is chosen for its simplicity and its ability to clearly illustrate the benefits of adaptive parameter selection.

Specifically, two parameter sets,  $(\alpha_1, \beta_1)$  and  $(\alpha_2, \beta_2)$ , are defined to correspond to high-rate and low-rate sampling regimes, respectively. The switching mechanism is driven by monitoring the magnitude of the product  $|f(t) f'(t)|$  in real time. When this quantity exceeds a prescribed threshold  $\delta$ , indicating a region of significant variation, the sampler operates in the high-rate mode using  $(\alpha_1, \beta_1)$ , where  $\alpha_1$  is small and  $\beta_1$  is large. Conversely, when  $|f(t) f'(t)| < \delta$ , the sampler switches to the low-rate mode with  $(\alpha_2, \beta_2)$ , where  $\alpha_2$  is larger and  $\beta_2$  is smaller, resulting in substantially reduced sampling density in slowly varying or flat regions.

Importantly, this adaptive modification does not alter the reconstruction algorithm, which remains identical to the fixed-parameter case. Consequently, the convergence guarantees of the reconstruction process are preserved, and perfect signal recovery remains possible without requiring any global upper bound on the inter-sample interval.

We evaluate the proposed adaptive strategy using the chirp bandlimited signal considered earlier. For these experiments, the parameters are set to  $(\alpha_1 = 0.09, \beta_1 = 2300)$  for the high-rate mode and  $(\alpha_2 = 0.9, \beta_2 = 10)$  for the low-rate mode, together with  $\delta = 6 \times 10^{-6}$ ,  $c = 1$  and  $s = 4.2c$ . The threshold  $\delta$  is chosen to be sufficiently small to ensure that the sampler switches to the low-rate regime only in regions where the signal exhibits negligible variation.

The reconstructed signal and the corresponding firing density are shown in Fig. 8. As evident from the firing density

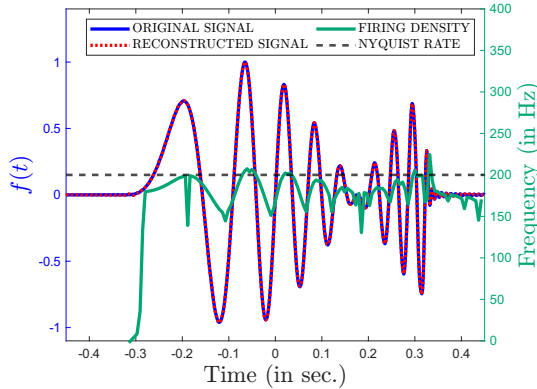


Fig. 8: Sampling and reconstruction using Adaptive-NUS with adaptive parameter selection;  $\#S = 136$ ; NMSE =  $-42.15$  dB.

plot, the sampling rate becomes extremely low in regions where the signal exhibits little or no variation, while increasing appropriately during periods of rapid change. Using this adaptive parameter strategy, the number of samples is reduced to 136, compared to 169 samples in the fixed-parameter adaptive scheme (cf. Fig. 4(c)). For most parts of the signal, the sampling rate remains below the Nyquist rate, with negligible sampling in flat regions. This reduction in sampling density comes at the cost of a modest increase in reconstruction error, with the NMSE increasing from  $-54$  dB to  $-42.15$  dB, where most of the error contribution arises from flat signal regions.

Finally, the proposed framework naturally admits further extensions. Additional parameter pairs  $(\alpha_i, \beta_i)$  and alternative switching rules may be incorporated in a systematic manner, enabling finer adaptation to signal dynamics and allowing the sampling scheme to be tailored to a broad range of signals and application scenarios.

## V. PRACTICAL APPLICATIONS

In this section, we demonstrate the applicability of the proposed adaptive non-uniform sampling framework to practical signal acquisition scenarios. We focus on two representative applications: ultrasonic guided-wave signals used in structural health monitoring (SHM) and electrocardiogram (ECG) signals.

### A. Ultrasonic Guided-Wave Signals

Motivated by recent developments in compact guided-wave-based SHM systems, we consider the ultrasonic pipeline monitoring framework reported in [50]. The experimental setup consists of a 4-inch-diameter steel pipe instrumented with eight torsional ultrasonic guided-wave transducers arranged circumferentially around the pipe. Each transducer is mounted using a  $10\text{ mm} \times 10\text{ mm}$  ring structure and can operate either as an actuator or as a sensor.

Damage assessment in such systems is typically performed by comparing the signals received at the transducers with a baseline signal acquired from the same structure under pristine conditions. Deviations between the received and baseline

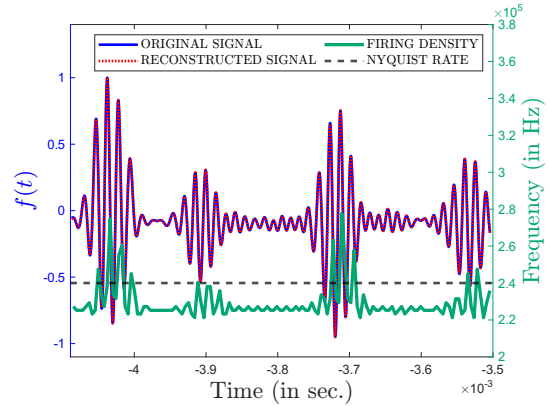


Fig. 9: Sampling and reconstruction of an ultrasonic guided-wave signal using the Adaptive-NUS method;  $\#S = 1856$ ; NMSE =  $-42.68$  dB.

signals are interpreted as indicators of potential structural anomalies.

We apply the proposed adaptive non-uniform sampling methodology directly to the guided-wave signals recorded by the receiving transducers, with the objective of reducing the sampling burden while preserving the signal characteristics required for reliable baseline comparison. For this experiment, the guided-wave signal has a bandwidth of  $1.2 \times 10^5$  Hz. The VBT-IF-TEM parameters are set to  $\alpha = 0.145$ ,  $\beta = 1.999 \times 10^{10}$ ,  $s = 4.2$ , and  $c = 1$ .

Fig. 9 illustrates the performance of the proposed scheme for ultrasonic guided-wave signals. The signal is sampled at a rate well below the Nyquist threshold while still allowing accurate reconstruction. Specifically, the adaptive sampling process generates 1856 samples, compared to 1966 samples required by uniform Nyquist sampling over the same duration. Despite this reduction in sampling density, the reconstructed signal achieves an NMSE of  $-42.68$  dB, indicating high reconstruction fidelity.

These results highlight the ability of the proposed adaptive sampling framework to exploit local signal structure, enabling sub-Nyquist sampling while maintaining accurate signal reconstruction in practical SHM applications.

### B. ECG Signals

We next evaluate the proposed VBT-IF-TEM framework on ECG signals, which are characterized by strong temporal structure and extended intervals of low activity interspersed with brief, high-variation events. These properties make ECG signals particularly well-suited for adaptive sampling strategies.

In this experiment, the ECG signal has a bandwidth of 100 Hz, and the VBT-IF-TEM parameters are set to  $\alpha = 0.15$ ,  $\beta = 5600$ ,  $s = 3.2$ , and  $c = 1.0$ . These results further demonstrate the effectiveness of the proposed adaptive framework for biomedical signals, where substantial temporal redundancy can be exploited to achieve efficient sampling without compromising reconstruction quality. Fig. 10 illustrates the application of the proposed scheme to an ECG signal. Due to the piecewise-smooth nature of the waveform, the adaptive sampler assigns a

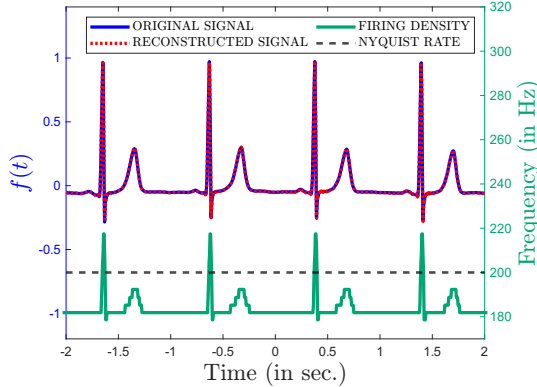


Fig. 10: Sampling and reconstruction of an ultrasonic guided-wave signal using the Adaptive-NUS method;  $\#S = 1837$ ; NMSE =  $-32.45\text{dB}$ .

higher sampling density to regions of rapid temporal variation, such as the QRS complexes, while significantly reducing the sampling density in flatter segments. As a result, the proposed method generates 1837 samples over the signal duration, compared to 2000 samples required by uniform Nyquist sampling. Despite this reduction in sampling load, the reconstructed ECG signal achieves an NMSE of  $-32.45$  dB, indicating accurate recovery under sub-Nyquist sampling conditions.

## VI. CONCLUSION

We presented an adaptive non-uniform sampling framework for bandlimited signals based on a locally adaptive sufficient condition for perfect reconstruction. By revisiting the convergence analysis of iterative reconstruction algorithms, we derived a local, energy-based bound that relaxes the need for a global Nyquist-type constraint and permits larger inter-sample intervals in slowly varying signal regions.

Guided by this analysis, we developed a variable-bias, variable-threshold integrate-and-fire time encoding machine that generates signal-dependent time encodings while preserving reconstruction guarantees. A biased-signal formulation was introduced to suppress excessive firing in low-energy regimes where the magnitude of the signal amplitude is small. Simulations and real-world experiments demonstrated that the proposed framework reduces sampling density compared to uniform sampling and conventional IF-TEMs while maintaining accurate reconstruction, and an adaptive parameter selection strategy illustrated how the sampling-accuracy tradeoff can be navigated in practice.

## REFERENCES

- [1] H. Nyquist, "Certain topics in telegraph transmission theory," *Trans. American Inst. of Elect. Eng.*, vol. 47, no. 2, pp. 617–644, Apr. 1928.
- [2] C. E. Shannon, "A mathematical theory of communication," *The Bell Syst. Tech. J.*, vol. 27, pp. 623–656, 1948.
- [3] Z.-P. Liang and P. C. Lauterbur, "Principles of magnetic resonance imaging: A signal processing perspective," *IEEE Press Series in Biomedical Engineering*, 1999, chapter on non-uniform sampling in NMR/MRI.
- [4] P. J. Beatty, D. G. Nishimura, and J. M. Pauly, "Rapid gridding reconstruction with a recursive, spatially oversampled fourier transform," *IEEE Trans. Medical Imaging*, vol. 24, no. 1, pp. 16–25, 2005.
- [5] H. J. Landau, "Necessary density conditions for sampling and interpolation of certain entire functions," *Acta Mathematica*, vol. 117, no. 1, pp. 37–52, 1967.
- [6] H. G. Feichtinger, K. Gröchenig, and T. Strohmer, "Efficient numerical methods in non-uniform sampling theory," *Nume. Math.*, vol. 69, pp. 423–440, 1995.
- [7] F. Marvasti, "Nonuniform sampling," in *Advanced topics in Shannon sampling and interpolation theory*. Springer, 1993, pp. 121–156.
- [8] K. Yao and J. Thomas, "On some stability and interpolatory properties of nonuniform sampling expansions," *IEEE Trans. Circuit Theory*, vol. 14, no. 4, pp. 404–408, 1967.
- [9] J. Yen, "On nonuniform sampling of bandwidth-limited signals," *IRE Trans. Circuit Theory*, vol. 3, no. 4, pp. 251–257, 1956.
- [10] A. A. Lazar and L. T. Tóth, "Perfect recovery and sensitivity analysis of time encoded bandlimited signals," *IEEE Trans Circuits and Syst. I: Regular Papers*, vol. 51, no. 10, pp. 2060–2073, 2004.
- [11] A. J. Kamath and C. S. Seelamantula, "Differentiate-and-fire time-encoding of finite-rate-of-innovation signals," in *Proc. IEEE Int. Conf. Acoust., Speech and Signal Process. (ICASSP)*, 2022, pp. 5637–5641.
- [12] A. Omar and A. Cohen, "Adaptive integrate-and-fire time encoding machine," in *Proc. European Signal Process. Conf. (EUSIPCO)*, 2024, pp. 2442–2446.
- [13] R. Alexandru, N. T. Thao, D. Rzepka, and P. L. Dragotti, "Sampling Classes of Non-Bandlimited Signals Using Integrate-and-Fire Devices: Average Case Analysis," in *Proc. IEEE Int. Conf. Acoust., Speech and Signal Process. (ICASSP)*. IEEE, 2020, pp. 9279–9283.
- [14] H. Naaman, S. Mulleti, Y. C. Eldar, and A. Cohen, "Time-based quantization for FRI and bandlimited signals," in *European Signal Process. Conf. (EUSIPCO)*, 2022, pp. 2241–2245.
- [15] H. Naaman, N. I. Bernardo, A. Cohen, and Y. C. Eldar, "Time encoding quantization of bandlimited and finite-rate-of-innovation signals," *IEEE Access*, 2025.
- [16] A. A. Lazar, "Time encoding with an integrate-and-fire neuron with a refractory period," *Neurocomputing*, vol. 58, pp. 53–58, 2004.
- [17] K. Adam, A. Scholefield, and M. Vetterli, "Sampling and reconstruction of bandlimited signals with multi-channel time encoding," *IEEE Trans. Signal Process.*, vol. 68, pp. 1105–1119, 2020.
- [18] D. Gontier and M. Vetterli, "Sampling based on timing: Time encoding machines on shift-invariant subspaces," *Applied and Comput. Harmonic Anal.*, vol. 36, no. 1, pp. 63–78, 2014.
- [19] H. Naaman, S. Mulleti, and Y. C. Eldar, "FRI-TEM: Time Encoding Sampling of Finite-Rate-of-Innovation Signals," *IEEE Trans. Signal Process.*, vol. 70, pp. 2267–2279, 2022.
- [20] R. Alexandru and P. L. Dragotti, "Reconstructing classes of non-bandlimited signals from time encoded information," *IEEE Trans. Signal Process.*, vol. 68, pp. 747–763, 2020.
- [21] D. Florescu and A. Bhandari, "Time encoding via unlimited sampling: Theory, algorithms and hardware validation," *IEEE Trans. Signal Process.*, vol. 70, pp. 4912–4924, 2022.
- [22] N. T. Thao and D. Rzepka, "Time encoding of bandlimited signals: Reconstruction by pseudo-inversion and time-varying multiplierless FIR filtering," *IEEE Trans. Signal Process.*, vol. 69, pp. 341–356, 2020.
- [23] A. J. Kamath and C. S. Seelamantula, "Multichannel time-encoding of finite-rate-of-innovation signals," in *Proc. IEEE Int. Conf. Acoust., Speech and Signal Process. (ICASSP)*. IEEE, 2023, pp. 1–5.
- [24] N. Fu, H. Zhang, S. Yun, Z. Wei, and L. Qiao, "Time-based finite-rate-of-innovation sampling for variable-pulse-width signal," *IEEE Trans. Inst. Meas.*, vol. 73, pp. 1–9, 2024.
- [25] D. Florescu, "A generalized approach for recovering time encoded signals with finite rate of innovation," *IEEE Trans. Signal Process.*, 2025.
- [26] N. I. Bernardo, "Symbol detection using an integrate-and-fire time encoding receiver," *arXiv preprint arXiv:2508.17704*, 2025.
- [27] R. J. Duffin and A. C. Schaeffer, "A class of nonharmonic Fourier series," *Trans. American Math. Soc.*, vol. 72, no. 2, pp. 341–366, 1952.
- [28] R. Wiley, "Recovery of bandlimited signals from unequally spaced samples," *IEEE Trans. Comm.*, vol. 26, no. 1, pp. 135–137, 1978.
- [29] F. Marvasti, M. Analoui, and M. Ghamshadzahi, "Recovery of signals from nonuniform samples using iterative methods," *IEEE Trans. Signal Process.*, vol. 39, no. 4, pp. 872–878, 1991.
- [30] K. Gröchenig, "Reconstruction algorithms in irregular sampling," *Mathematics of computation*, vol. 59, no. 199, pp. 181–194, 1992.
- [31] H. G. Feichtinger and K. Gröchenig, "Theory and practice of irregular sampling," in *Wavelets*. CRC Press, 2021, pp. 305–363.
- [32] W. Sun and X. Zhou, "Reconstruction of band-limited signals from local averages," *IEEE Trans. Info. Theory*, vol. 48, no. 11, pp. 2955–2963, 2002.

- [33] Z. Song, B. Liu, Y. Pang, C. Hou, and X. Li, "An improved Nyquist–Shannon irregular sampling theorem from local averages," *IEEE Trans. Info. Theory*, vol. 58, no. 9, pp. 6093–6100, 2012.
- [34] S.-H. Li and W. Lin, "Remarks on the Voronoi method in Paley–Wiener space," *J. Mathematical Ana. Appl.*, vol. 318, no. 1, pp. 1–14, 2006.
- [35] B. F. Logan Jr, "Information in the zero crossings of bandpass signals," *Bell Syst. Technical J.*, vol. 56, no. 4, pp. 487–510, 1977.
- [36] J. Mark and T. Todd, "A nonuniform sampling approach to data compression," *IEEE Trans. Comm.*, vol. 29, no. 1, pp. 24–32, 1981.
- [37] N. Sayiner, H. V. Sorensen, and T. R. Viswanathan, "A level-crossing sampling scheme for A/D conversion," *IEEE Trans. Circuits Syst. II: Analog Digital Signal Process.*, vol. 43, no. 4, pp. 335–339, 1996.
- [38] H. Boche and U. J. Mönich, "Towards a general theory of reconstruction of bandlimited signals from sine wave crossings," *Signal Process.*, vol. 92, no. 3, pp. 737–751, 2012.
- [39] D. Rzepka, M. Miśkowicz, D. Kościelnik, and N. T. Thao, "Reconstruction of signals from level-crossing samples using implicit information," *IEEE Access*, vol. 6, pp. 35001–35011, 2018.
- [40] Y. Tsividis, "Event-driven data acquisition and digital signal processing— A tutorial," *IEEE Trans. Circuits Syst. II, Exp. Briefs*, vol. 57, no. 8, pp. 577–581, 2010.
- [41] P. Martínez-Nuevo, H.-Y. Lai, and A. V. Oppenheim, "Amplitude sampling," in *Allerton Conf. Comm. Ctr. Comput. (Allerton)*. IEEE, 2016, pp. 17–22.
- [42] J. Clark, M. Palmer, and P. Lawrence, "A transformation method for the reconstruction of functions from nonuniformly spaced samples," *IEEE Tran. Acoustics, Speech, Signal Process.*, vol. 33, no. 5, pp. 1151–1165, 1985.
- [43] T. G. Dvorkind, Y. C. Eldar, and E. Matusiak, "Nonlinear and nonideal sampling: Theory and methods," *IEEE Trans. Signal Process.*, vol. 56, no. 12, pp. 5874–5890, 2008.
- [44] K. Horiuchi, "Sampling principle for continuous signals with time-varying bands," *Info. Control*, vol. 13, no. 1, pp. 53–61, 1968.
- [45] D. Wei and A. V. Oppenheim, "Sampling based on local bandwidth," in *Asilomar Conf. Signals, Syst. Comput.*. IEEE, 2007, pp. 1103–1107.
- [46] D. Rzepka and M. Miśkowicz, "Recovery of varying-bandwidth signal from samples of its extrema," in *Signal Processing: Algo. Architectures Arrangements, Appl.(SPA)*. IEEE, 2013, pp. 143–148.
- [47] B. Andreolli and K. Gröchenig, "Sampling theorems in spaces of variable bandwidth generated via wilson basis," in *Proc. Intl. Conf. Sampling theory and Appl. (SampTA)*. IEEE, 2023, pp. 1–5.
- [48] A. Omar and A. Cohen, "Adaptive integrate-and-fire time encoding machine," in *European Signal Process. Conf. (EUSIPCO)*. IEEE, 2024, pp. 2442–2446.
- [49] A. Arora and S. Mulleti, "A lowrate variable-bias integrate-and-fire time encoding machine," in *IEEE Int. Conf. Acoust., Speech and Signal Process. (ICASSP)*, 2025, pp. 1–5.
- [50] S. Patil, S. Banerjee, and S. Tallur, "Smart structural health monitoring (shm) system for on-board localization of defects in pipes using torsional ultrasonic guided waves," *Scientific Reports*, vol. 14, no. 1, p. 24455, 2024.